Property Influence of Polyanilines on Photovoltaic Behaviors of Dye-Sensitized Solar Cells

Shuxin Tan,[†] Jin Zhai,*[,†] Bofei Xue,[‡] Meixiang Wan,[†] Qingbo Meng,*[,‡] Yuliang Li,[†] Lei Jiang,[†] and Daoben Zhu[†]

Center for Molecular Science, Institute of Chemistry, Chinese Academy of Sciences, Beijing 100080, China, and State Key Laboratory for Surface Physics, Institute of Physics, Chinese Academy of Sciences, Beijing 100080, China

Received December 2, 2003. In Final Form: January 12, 2004

The influence of polyanilines (PANIs) as hole conductors on the photovoltaic behaviors of dye-sensitized solar cells is studied. The current−voltage (*I*−*V*) characteristics and the incident photon to current conversion efficiency (IPCE) curves of the devices are determined as the function of different conductivities and morphologies of PANIs. The results show that the conductivity of PANIs affects the performance of the devices greatly, and PANI with the intermediate conductivity value (3.5 S/cm) is optimum. In addition, the effects of both the film formation property and the cluster size of polyanilines on the photovoltaic behaviors of the devices are also discussed.

Introduction

The dye-sensitized solar cell (DSSC) based on the nanoporous TiO_2 electrode[1−5] is of great interest since Grätzel and co-workers reported it in 1991 because of its relatively low cost and reasonably high efficiency compared with the conventional Si or GaAs cell. In the system of DSSCs, a dye molecule absorbs visible light and, after excitation, injects electrons into the conduction band of TiO_2. Thus, the dye becomes oxidized. Such state is reduced by an electrolyte, and the electrolyte finally gets electrons from the counter electrode.[1−5] Although the energy conversion efficiency (η_e) of such a system with liquid electrolyte reaches as high as 10%,[6−9] the device has significant technological problems including sealing and stability. It is proved that solid analogues (i.e., hole conductors), such as inorganic p-type semiconductors (CuI and CuSCN)[11−16] and the amorphous organic hole conducting material (2,2′,7,7′-tetrakis(*N*,*N*-di-*p*-methoxyphenyl-amine)-9,9′-spirobifluorene),[10,17] can avoid the above-mentioned problems and, hence, are promising materials to replace liquid electrolytes.[10−12]

Recently, many efforts in hole conductor research are focusing on conducting polymers, because they are inexpensive and can be tailored chemically to fit a wide range of purposes. For example, polythiophene, polypyrrole, polyphenylenevinylene (PPV), polyaniline, and their derivatives are all used as hole conductors for fabrication of DSSCs.[5,18−26] It is considered that conductivity and pore filling of the conducting polymers are two main factors influencing the photovoltaic behaviors of devices. In this work, the influences of the conductivity, film formation property, and cluster size of the polyanilines (PANIs) as hole conductors on the photovoltaic behaviors of the DSSCs are studied.

Experimental Section

Hole Conductor Materials. Several PANIs with different conductivities, signaled by EB, ES_1, ES_2, ES_3, and ES_4, are used as hole conductors. Their compositions and conductivities are

* To whom correspondence should be addressed. E-mail: zhaijin@iccas.ac.cn (Jin Zhai) and qbmeng@aphy.iphy.ac.cn (Qingbo Meng).

[†] Center for Molecular Science.

[‡] State Key Laboratory for Surface Physics.

(1) O'Regan, B.; Grätzel, M. *Nature* **1991**, *353*, 737.
(2) Stathatos, E.; Lianos, P.; Krontiras, C. *J. Phys. Chem. B* **2001**, *105*, 3486.
(3) Cao, F.; Oskam, G.; Searson, P. C. *J. Phys. Chem.* **1995**, *99*, 17071.
(4) Tennakone, K.; Senadeera, G. K. R.; Perea, V. P. S.; Kottegoda, I. R. M.; De Silva, L. A. A. *Chem. Mater.* **1999**, *11*, 2474.
(5) Arango, A. C.; Johnson, L. R.; Bliznyuk, V. N.; Schlesinger, Z.; Carter, S. A.; Horhold, H.-H. *Adv. Mater.* **2000**, *12*, 1689.
(6) Nazeeruddin, M. K.; Pechy, P.; Renouard, T.; Zakeeruddin, S. M.; Hurnphry-Baker, R.; Comte, P.; Liska, P.; Cevery, L.; Costa, E.; Shklover, V.; Spiccia, L.; Deacon, G. B.; Bignozzi, C. A.; Grätzel, M. *J. Am. Chem. Soc.* **2001**, *123*, 1613.
(7) Nazeeruddin, M. K.; Grätzel, M. *J. Photochem. Photobiol., A* **2001**, *145*, 79.
(8) Grätzel, M. *J. Photochem. Photobiol., C* **2003**, *4*, 145.
(9) Wang, Z.-S.; Huang, C.-H.; Huang, Y.-Y.; Hou, Y.-J.; Xie, P.-H.; Zhang, B.-W.; Cheng, H.-M. *Chem. Mater.* **2001**, *13*, 678.
(10) Bach, U.; Lupo, D.; Comte, P.; Moser, J. E.; Weissörtel, F.; Salbeck, J.; Spreitzer, H.; Grätzel, M. *Nature* **1998**, *395*, 583.
(11) Kumara, G. R. R. A.; Kaneko, S.; Okuya, M.; Tennakone, K. *Langmuir* **2002**, *18* (26), 10493.
(12) O'Regan, B.; Schwartz, D. T.; Zakeeruddin, S. M.; Grätzel, M. *Adv. Mater.* **2000**, *12*, 1263.
(13) Kumara, G. R. R. A.; Konno, A.; Shiratsuchi, K.; Tsukahara, J.; Tennakone, K. *Chem. Mater.* **2002**, *14*, 954.
(14) Kumara, G. R. R. A.; Konno, A.; Senadeera, G. K. R.; Jayaweera, P. V. V.; De Silva, D. B. R. A.; Tennakone, K. *Sol. Energy Mater. Sol. Cells* **2001**, *69*, 195.
(15) O'Regan, B.; Schwartz, D. T. *Chem. Mater.* **1995**, *7*, 1349.
(16) Meng, Q.-B.; Takahashi, K.; Zhang, X.-T.; Sutanto, I.; Rao, T. N.; Sato, O.; Fujishima, A.; Watanabe, H.; Nakamori, T.; Uragami, M. *Langmuir* **2003**, *19*, 3572.
(17) Krüger, J.; Plass, R.; Cevey, L.; Piccirelli, M.; Grätzel, M.; Bach, U. *Appl. Phys. Lett.* **2001**, *79*, 2085.
(18) Gebeyehu, D.; Brabec, C. J.; Sariciftci, N. S. *Thin Solid Films* **2002**, *403*−*404*, 271.
(19) Gebeyehu, D.; Brabec, C. J.; Sariciftci, N. S.; Vangeneugden, D.; Kiebooms, R.; Vanderzande, D.; Kienberger, F.; Schindler, H. *Synth. Met.* **2002**, *125*, 279.
(20) Spiekermann, S.; Smestad, G.; Kowalik, J.; Tolbert, L. M.; Grätzel, M. *Synth. Met.* **2001**, *121*, 1603.
(21) Murakoshi, K.; Kogure, R.; Wada, Y.; Yanagida, S. *Chem. Lett.* ***1997***, *26* (5), 471.
(22) Tennakone, K.; Kumara, G. R. R. A.; Kottegoda, I. R. M.; Wijayantha, K. G. U.; Perera, V. P. S. *J. Phys. D*: *Appl. Phys.* **1998**, *31*, 1492.
(23) Kajihara, K.; Tanaka, K.; Hirao, K.; Soga, N. *Jpn. J. Appl. Phys.* **1997**, *56*, 5537.
(24) Van Hal, P. A.; Christiaans, M. P. T.; Wienk, M. M.; Kroon, J. M.; Janssen, R. A. J. *J. Phys. Chem. B* **1999**, *103*, 4352.
(25) Tan, S. X.; Zhai, J.; Wan, M. X.; Jiang, L.; Zhu, D. B. *Synth. Met.* **2003**, *137*, 1511.
(26) Senadeera, G. K. R.; Kitamura, T.; Wada, Y.; Yanagida, S. XXIst International Conference on Photochemistry, Nara, Japan, 2003.

10.1021/la036260m CCC: $27.50
Published on Web 02/17/2004

Table 1. Chemical Compositions and Corresponding Conductivities (σ) of PANIs Used as Hole Conductors in This Work

PANIs	components	σ (S/cm)
EB	emeraldine base in *N*-methylpyrrolidinone	$\sim 10^{-7}$
ES_1	mixture of EB and ES_4	$\sim 10^{-3}$
ES_2	4-dodecylbenzenesulfonic acid doped polyaniline in chloroform	3.5
ES_3	mixture of ES_2 and ES_4	131
ES_4	10-camphorsulfonic acid doped PANI in *m*-cresol	297

Chart 1. Chemical Structures of PANIs: (a) EB ($\sigma \approx 10^{-7}$ S/cm); (b) ES_2 ($\sigma = 3.5$ S/cm) and ES_4 ($\sigma = 297$ S/cm)

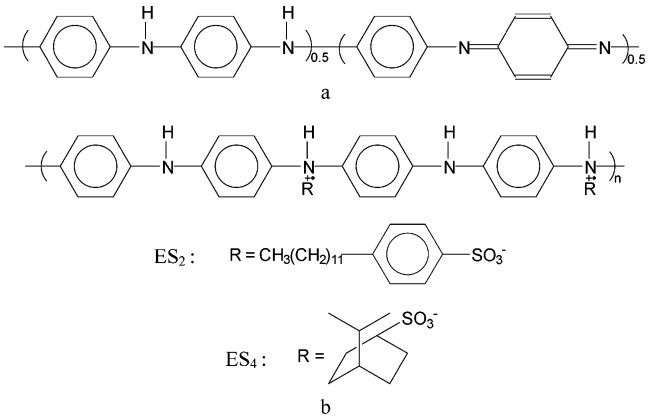

listed in Table 1. EB, ES_2, and ES_4 are represented as the emeraldine base form of PANI dissolved in *N*-methylpyrrolidinone, 4-dodecylbenzenesulfonic acid (DBSA) doped PANI in chloroform, and 10-camphorsulfonic acid (CSA) doped PANI in *m*-cresol, respectively. ES_1 is a mixture of EB and ES_4. ES_3 is composed of ES_2 and ES_4. The chemical structures of EB, ES_2, and ES_4[27−30] are given in Chart 1. Their synthetic methods can be found elsewhere.[31−34]

Fabrication of Devices. All DSSCs were fabricated as below. First, the TiO_2 barrier layer was deposited on the surface of the fluorine-doped conducting tin oxide (FTO) glass substrate (the sheet resistance is ca. 30 Ω/□) by spin-coating a solution containing 4 mL of titanium isopropoxide and 40 mL of ethanol twice. Then the nanoporous TiO_2 film was prepared according to the following procedure. Titanium isopropoxide (Aldrich, 5 mL), glacial acetic acid (homemade, 5.5 mL), 2-propanol (homemade, 10 mL), water (3 mL), and TiO_2 powder (Millennium Chemicals, PC 500, 0.65 g) were added into a mortar and ground to form a slurry. The slurry was spread and allowed to dry on the surface of the barrier layer at 120 °C. Then the substrate was sintered at 450 °C for 10 min. This process was repeated until a fully covered translucent film was deposited.[14]

By immersion of the above film into 2×10^{-4} M *cis*-di-(isothiocyanato)-*N*-bis(4,4′-dicarboxy-2,2′-bipyridine) ruthenium-(II) dye (N3, Solaronix SA) ethanol solution overnight, a dye-sensitized nanocrystalline TiO_2 film was formed. Then the PANI solution was dropped onto the film. After the film dried, another cleaned FTO glass was clipped onto the top of the as-prepared PANI layer to form a solar cell. All cells were produced under ambient conditions.

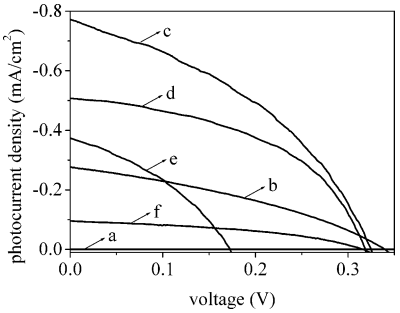

Figure 1. Current−voltage ($I-V$) characteristics of the dye-sensitized TiO_2 solar cells with active area of 0.2 cm^2 under 100 mW/cm^2 illumination using different PANIs as hole conductors: (a) TiO_2/dye/EB ($\sigma \approx 10^{-7}$ S/cm); (b) TiO_2/dye/ES_1 ($\sigma \approx 10^{-3}$ S/cm); (c) TiO_2/dye/ES_2 ($\sigma = 3.5$ S/cm); (d) TiO_2/dye/ES_3 ($\sigma = 131$ S/cm); (e) TiO_2/dye/ES_4 ($\sigma = 297$ S/cm); (f) TiO_2/ES_2 ($\sigma = 3.5$ S/cm).

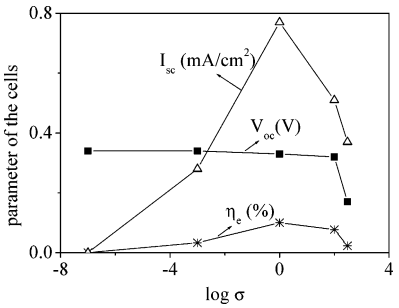

Figure 2. The relationships of the open-circuit voltage (V_{oc}), short-circuit current (I_{sc}), and overall solar-to-electrical energy conversion efficiency (η_e) with the conductivity (σ) of PANIs.

Measurements. The current−voltage ($I-V$) characteristics of the devices were recorded with an electrochemical analyzer (CHI630A, Chenhua Instruments Co., Shanghai) under illumination of 100 mW/cm^2 white light from a solar simulator (CMH-250, Aodite Photoelectronic Technology Ltd., Beijing). The incident photon to current conversion efficiency (IPCE) curves of the devices were measured, and monochromatic light was obtained by passing light through a series of light filters with different wavelengths. The conductivities of different PANIs were determined by a four-electrode system.[35] The UV−vis spectra were obtained by a spectrophotometer (U-3010, Hitachi). The surface morphologies of the films were investigated by scanning electron microscopy (JSM-6700F, JEOL).

Results and Discussion

***I−V* Characteristics.** Figure 1a−e shows $I-V$ curves of DSSCs with five PANIs as hole conductors under 100 mW/cm^2 illumination. The relationships of open-circuit voltage (V_{oc}), short-circuit current density (I_{sc}), and overall solar-to-electrical energy conversion efficiency (η_e) with the conductivity of PANIs are presented in Figure 2. It can be seen that I_{sc} and η_e increase with the increase of conductivity to 3.5 S/cm and then drop down. The maximum I_{sc} and η_e are 0.77 mA/cm^2 and 0.10%, respectively. The V_{oc} decreases slightly from 0.34 to 0.32 V with the increase of the conductivity from $\sim 10^{-7}$ to 131 S/cm but decreases sharply to 0.17 V at the conductivity of 297 S/cm. These results indicate that the intermediate conductivity of PANI in the semiconductor region is more suitable than those close to the conductor or in the insulator regions. The $I-V$ characteristics for the heterojunction of TiO_2/ES_2 under 100 mW/cm^2 illumination were also measured (Figure 1f) and showed much lower I_{sc} (0.09 mA/cm^2) and V_{oc} (0.32 V).

(27) Zhu, D.; Wang, F. *Organic Solids*; Science and Technology Publisher of Shanghai: Shanghai, China, 1999; Vol. 3, p 92.
(28) Avlyanov, J. K.; Min, Y.; MacDiarmid, A. G.; Epstein, A. J. *Synth. Met.* **1995**, *72*, 65.
(29) Tang, B. Z.; Geng, Y.; Lam, J. W. Y.; Li, B.; Jing, X.; Wang, X.; Wang, F.; Pakhomov, A. B.; Zhang, X. X. *Chem. Mater.* **1999**, *11*, 1581.
(30) Gettinger, C. L.; Heeger, A. J.; Pine, D. J.; Cao, Y. *Synth. Met.* **1995**, *74*, 81.
(31) MacDiarmid, A. G.; Chiang, J. D.; Ritcher, A. F.; Somasiri, N. L. D.; Epstein, A. J. *Conducting Polymers*; Alcacer, L., Ed.; D. Reidel: Dordrecht, The Netherlands, 1987.
(32) Cao, Y.; Smith, P.; Heeger, A. J. *Synth. Met.* **1992**, *48*, 91.
(33) Li, Y. M.; Wan, M. X. *Acta Polym. Sin.* **1998**, *2*, 177.
(34) Li, Y. M.; Wan, M. *J. Funct. Polym.* **1998**, *11*, 337.
(35) Wan, M. X.; Li, W. *J. Polym. Sci., Part A: Polym. Chem.* **1997**, *35*, 2129.

Chart 2. Schematic Diagram of the Dye-Sensitized TiO_2 Solar Cells

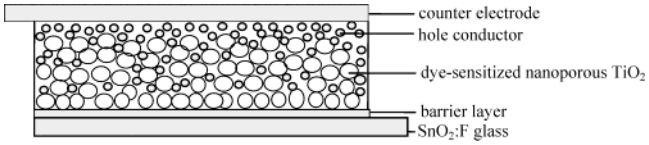

The photovoltaic behaviors of solar cells can be evaluated by the parameters of V_{oc}, I_{sc}, and η_e. V_{oc} is determined by the difference (ΔV) between the quasi-Fermi energy level of the TiO_2 (under illumination) and the highest occupied molecular orbital (HOMO) energy level of p-type conductors.[19,36] The cyclic voltammograms of EB, ES_2, and ES_4 (Supporting Information, Figure 1) show that the first oxidation peak shifts negatively with the increase of the conductivity, which leads to the promotion of the HOMO energy level and reduction of ΔV.[37] Simultaneously, the band gap of PANIs is reduced when the conductivity increases.[38] Thus, these may lead to the decrease of V_{oc}.[19,36,38−41] Furthermore, V_{oc} can also be reduced with the decrease of shunt resistance of the device.[42] In the system of DSSCs, the lower shunt resistance means the easier charge recombination of injected photoelectrons with the oxide hole conductor,[43] which is related to the higher conductivity of the hole conductor. In view of all the above-mentioned reasons, it can be well understood that V_{oc} of the device with ES_4 as the hole conductor is the lowest.

I_{sc} is proportional to the conductivity of the polymer, because the increase of conductivity accelerates the hole transfer rate in the polymer and reduces the inherent resistance of the device. At the same time, the short-circuiting loss between the hole collector and the conducting glass increases when the conductivity of the hole conductor is as high as that of metal. As a result, I_{sc} reaches a maximum when the conductivity of PANI has an intermediate value.

Morphology. Both the pore filling extent of the hole conductor into the dye-sensitized TiO_2 film and the electric contact of the hole conductor with the counter electrode are two important factors to influence the photovoltaic behaviors by changing the charge injection and transfer.[13,17−20] To demonstrate these factors vividly, a schematic diagram of the solid-state device is shown in Chart 2. The hole conductor may not penetrate all pores of dye-sensitized TiO_2 film, and the pore filling is correlated with the size of the hole conductor and the pores of dye-sensitized TiO_2 film. On the other hand, the electric contact of the hole conductor with the counter electrode is related to the surface smoothness of the hole conductor. Therefore, the surface morphologies and the cluster size of PANI films on dye-sensitized TiO_2 and dye-sensitized TiO_2 film are studied, and their scanning electron microscopy (SEM) images are shown in Figure 3. For ES_4 (Figure 3a), the

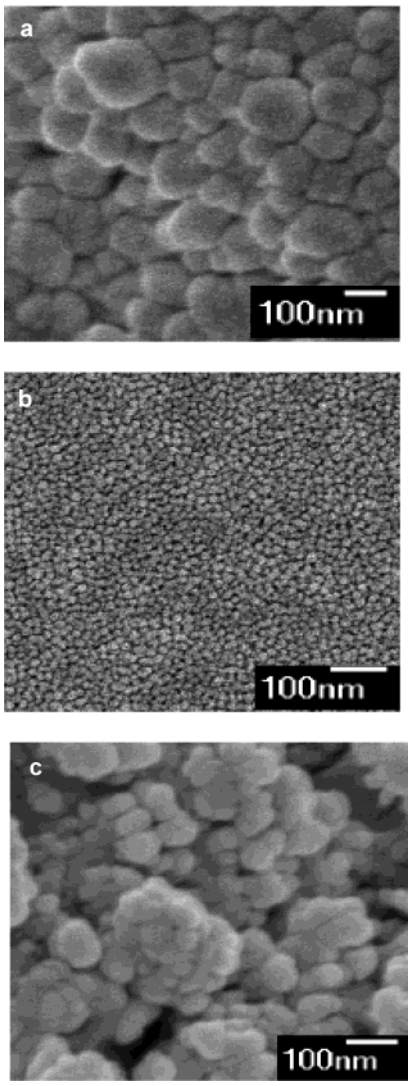

Figure 3. SEM images of different PANI coatings on dye-sensitized TiO_2 films (a,b) and dye-sensitized TiO_2 film without PANI coatings (c): (a) ES_4 (σ = 297 S/cm); (b) ES_2 (σ = 3.5 S/cm).

surface is rough, and there are many islands and clusters with the size of several hundred nanometers, even larger than that of the pores of the dye-sensitized TiO_2 electrode. The surfaces of EB, ES_1, and ES_3 (Supporting Information, Figure 2) are smoother than that of ES_4, containing a few isolated islands with the average size of 50 nm, which are composed of clusters from 10 to 20 nm. The surface of ES_2 (Figure 3b) is homogeneous and smooth with most uniform clusters of ca. 13 nm, showing the best film formation property. It can be inferred that the larger the clusters of PANIs, the greater the difficulty in filling them into the pores of dye-sensitized TiO_2 film. The rougher the surface, the more large-area defects and pinholes on PANI films exist. All of these cause the contact area between polymer and dye-sensitized TiO_2 or between polymer and counter electrode to be smaller. The poor pore filling and electric contact retard both the transport of photoelectrons from counter electrode to hole conductor and the regeneration of dye by the reduced-state hole conductor. This hindrance accelerates the recombination of photoelectrons injected into the conduction band of TiO_2 with the oxidized-state dye[19,44−45] and enhances the internal resistance of the

(36) Arango, A. C.; Carter, S. A.; Brock, P. J. *Appl. Phys. Lett.* **1999**, *74*, 1698.
(37) Zhang, W.; Shi, Y.; Gan, L.; Huang, C.; Luo, H.; Wu, D.; Li, N. *J. Phys. Chem. B* **1999**, *103*, 675.
(38) *Conducting Macromolecule Materials*; Sasabe, H., Ed.; Science Publisher: Beijing, China, 1989 (translated by Y. Cao and C. Ye).
(39) Melby, L. R.; Harder, R. J.; Hertler, W. R.; Mahler, W.; Benson, R. E.; Mochel, W. E. *J. Am. Chem. Soc.* **1962**, *84*, 3374.
(40) Morinaga, M.; Nogami, T.; Kanda, Y.; Matsumoto, T.; Matsuoka, K.; Mikawa, H. *Bull. Chem. Soc. Jpn.* **1980**, *53*, 1221.
(41) Cowan, D. O.; LeVande, C.; Park, J.; Kaufman, F. *Acc. Chem. Res.* **1973**, *6*, 1.
(42) Liu, E. *Photovoltaics and the Application*; Science Publisher: Beijing, China, 1989; Vol. 3, p 101.
(43) Gregg, B.-A.; Pichot, F.; Ferrere, S.; Fields, C. L. *J. Phys. Chem. B* **2001**, *105*, 1422.
(44) Nogueira, A. F.; Durrant, J. R.; De Paoli, M. A. *Adv. Mater.* **2001**, *13*, 826.

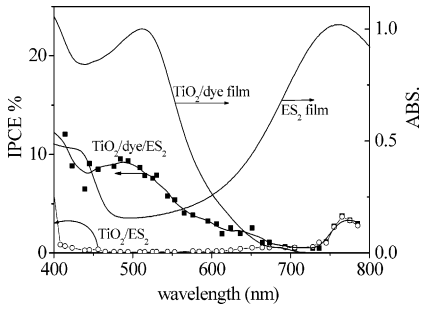

Figure 4. The IPCE curves (left) of dye-sensitized TiO_2 solar cells with ES_2 as the hole conductor (TiO_2/dye/ES_2) and the heterojunction of TiO_2/ES_2 without dye sensitization. The absorption spectra of dye-sensitized TiO_2 (TiO_2/dye) and ES_2 films (right).

device. Therefore, small uniform clusters and a good homogeneous surface of ES_2 are beneficial to the pore filling and, meanwhile, improve the electronic contact of the device.

IPCE and UV−Vis Spectra. The IPCE curves of the solar cells with ES_2 as the hole conductor are shown in Figure 4 (left). The maximum IPCE value of the dye-sensitized device approaches 10% at about 500 nm, corresponding to the absorption peak of the N_3 dye-sensitized TiO_2 film (Figure 4, right). In addition, there are photocurrent responses between 650 and 800 nm for both the dye-sensitized solar cell with ES_2 as the hole conductor and the heterojunction of TiO_2/ES_2, which is due to the sensitization of PANI because N_3 dye has no absorption at those wavelengths while ES_2 has (Figure 4, right). All these phenomena indicate that the photocurrent response can be attributed to the sensitization of both N_3 dye and PANI; that is, N_3 dye is the dominating sensitizer and PANI acts as not only a solid-state electrolyte but also a sensitizer.

(45) Nogueira, A. F.; De Paoli, M.-A.; Montanari, I.; Monkhouse, R.; Nelson, J.; Durrant, J. R. *J. Phys. Chem. B* **2001**, *105*, 7517.

Conclusions

In summary, the conductivity of PANIs has great influence on the photovoltaic behaviors of dye-sensitized solar cells. At the conductivity of 3.5 S/cm, the largest values of I_{sc} (0.77 mA/cm^2) and η_e (0.10%) are obtained, and the maximum IPCE value approaches 10%. When the conductivity is lower, the I_{sc} obviously decreases because lower conductivity leads to slower charge transport and higher series resistance of the device. On the contrary, when the conductivity is much higher (as high as 10^2 S/cm), the I_{sc} and V_{oc} both decrease due to the short-circuiting loss between the counter electrode and PANIs. This indicates that a conducting polymer with appropriate conductivity in the semiconductor region is better than those close to insulator or metal. At the same time, the influence of the film formation property and cluster size of polymers on the performance of the devices is deduced. It can be concluded that a conducting polymeric material with large band gap, sufficient conductivity, homogeneous surface, and small size of clusters is desirable as a hole conductor in DSSCs.

Acknowledgment. This work was supported by the State Key Project for Fundamental Research (G199906-4504), the Hi-Tech Research and Development program of China (863 Project, 2002AA302403), and the Special Research Foundation of the National Natural Science Foundation of China (20125102). The authors thank Professor A. Fujishima at the University of Tokyo, Japan, for his warmhearted help.

Supporting Information Available: Cyclic voltammograms of EB, ES_2, and ES_4 films; SEM images of different PANI coatings on dye-sensitized TiO_2 films. This material is available free of charge via the Internet at http://pubs.acs.org.

LA036260M